REVISTA INTERDISCIPLINAR DE PESQUISA EM ENGENHARIA

CILAMCE 2016

XXXVII IBERIAN LATIN AMERICAN CONGRESS ON COMPUTATIONAL METHODS IN ENGINEERING

BRASÍLIA - DF - BRAZIL

MICROMECHANICAL APPROACH TO VISCOELASTIC BEHAVIOR OF FRACTURED MEDIA

Cássio B. de Aguiar

Samir Maghous

cassio.barros.aguiar@gmail.com

samir.maghous@ufrgs.br

Universidade Federal do Rio Grande do Sul

Av. Osvaldo Aranha, 99 – Centro Histórico, 90035-190, Rio Grande do Sul, Porto Alegre, Brazil

Abstract. *This paper presents a micromechanical approach to overall viscoelastic properties of randomly fractured media. Unlike cracks, fractures can be viewed as interfaces that are able to transfer efforts. Their specific behavior under shear and normal stresses is a fundamental component of the deformation and fracture in brittle materials such as geomaterials. Based on the implementation of the Mori-Tanaka linear homogenization scheme, the first part of the analysis is dedicated to derive close-form expressions for the homogenized elastic stiffness tensor of the fractured medium. The effective viscoelastic behavior is then assessed from the elastic homogenization in Laplace framework and making use of the correspondence principle. In this context, a specific procedure for performing the inverse of Carson-Laplace transform is developed, allowing for the analytical derivation of homogenized relaxation and creep tensors. It is shown that the viscoelastic behavior can generally be described by means of a generalized Maxwell rheological model. For practical implementation in structural analyses, an approximation of the effective behavior by a Burger–like model is formulated in the last part of the paper.*

Keywords: *Fractures, Micromechanics, Viscoelasticity.*

1 INTRODUCTION

A main characteristic of many engineering materials such as rocks and more generally geomaterials, is the presence at different scales of discontinuities (cracks or fractures). The term "fracture" refers to a zone of small thickness along which the mechanicals properties of the matrix material are significantly degraded. Strength, deformability and conductivity of fractured media are strongly affected by the presence of these discontinuities (e.g. Barton et al., 1985; Maghous et al., 2008).

Most of the theoretical or computational analyses investigating the mechanical behavior of cracked or fractured media have focused on the modeling of their instantaneous (elastic or plastic) response, whereas few works dealt with delayed (time-dependent) behavior of such materials are available in literature. In the framework of non-aging linear viscoelasticity, Le et al. (2008) proposed a reasoning to the multi-scales modeling of heterogeneous materials. Using the correspondence principle coupled with the Eshelby-based homogenization schemes, Le et al. establish an equivalent model to the viscoelastic heterogeneous material. However, this analysis was limited to classical heterogeneities. Nguyen (2010) and Nguyen et al. (2011, 2013) were extend this approach to cracked media, developing a micromechanics-based model for viscoelastic medium where the heterogeneities are cracks. These authors formulated a three-dimensional Burger model to approximate the homogenized viscoelastic behavior. Nevertheless, the analysis has been restricted to viscoelastic materials with cracks (i.e., discontinuities without stress transfers reduced to cracks). The present paper is conceived as an extension of the Nguyen's analysis, adding the behavior of fractures, studied by Maghous et al. (2011), that are discontinuities able to transfer stresses.

2 ELASTIC BEHAVIOR OF FRACTURED MATERIALS

To formulate the delayed behavior of the fractured material, the first step shall consist in formulating the instantaneous elastic behavior. The stating point is the micromechanics-based approach originally developed in Maghous et al. (2011) and extended later in Maghous et al. (2014) to evaluate in the context of elasticity the homogenized behavior of a medium with an isotropic distribution of fractures (or discontinuities). The main features of the latter approach are briefly recalled in the sequel.

It is first emphasized that fractures can be viewed as cracks that are able to transfer normal as well as tangential stresses. They are classically modeled as interfaces with attached orthonormal frame $\left(\underline{t}, \underline{t}', \underline{n}\right)$ (see Fig. 1) and whose behavior is described by means of a relationship relating the stress vector $\underline{T} = \underline{\underline{\sigma}} \cdot \underline{n}$ acting on the joint and the corresponding relative displacement $[\underline{\xi}]$:

$$\underline{T} = \underline{\underline{k}} \cdot [\underline{\xi}] \qquad \text{with} \quad \underline{\underline{k}} = k_n \, \underline{n} \otimes \underline{n} + k_t \left(\underline{t} \otimes \underline{t} + \underline{t}' \otimes \underline{t}'\right) \tag{1}$$

The stiffness $\underline{\underline{k}}$ is defined by the scalars k_n and k_t referring to the normal and shear stiffness of the fracture, respectively.

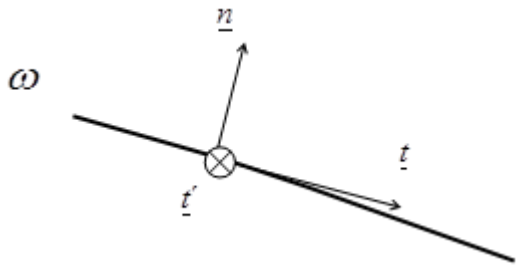

Figure 1. Local frame for joint ω modeled as an interface

The intact matrix is assumed to be linearly elastic with fourth-order stiffness tensor $\mathbb{C}_s$ relating the local stress and strain: $\underline{\underline{\sigma}} = \mathbb{C}_s : \underline{\underline{\varepsilon}}$.

The homogenized (effective) elastic behavior of the fractured medium is assessed applying the framework of Eshelby-based homogenization schemes (e.g. Dormieux et al., 2006). For this purpose, an appropriate geometrical description of the fracture should be adopted. the fractures are represented by oblate spheroids with attached orthonormal frame $\left(\underline{t}, \underline{t}', \underline{n}\right)$ (see Fig. 2).

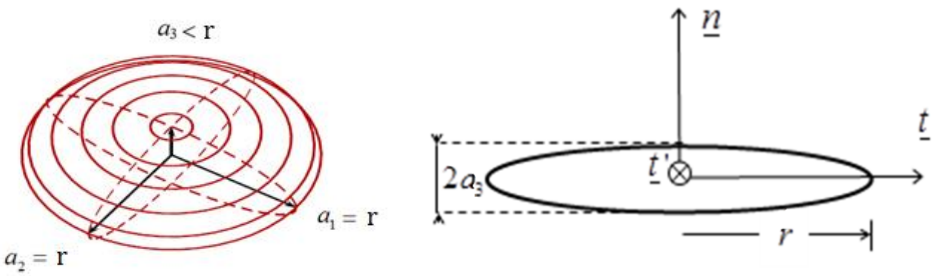

Figure 2. Local frame for joint ω modeled as an interface

The radius of the oblate is r and the half opening is a_3. The aspect ratio $\mathrm{X} = a_3 / r$ of such a penny-shaped crack is subjected to the condition $\mathrm{X} << 1$. In the continuum micromechanics approach employed herein, a fracture represents an inhomogeneity embedded within the intact matrix. The matrix stiffness is $\mathbb{C}_s$ and the fracture stiffness is $\underline{\underline{k}}$. In this context, the elastic material takes the place of the matrix and the fractures takes the place of the heterogeneities. The volume fraction of fractures in the medium is denoted by f :

$$f = \frac{4}{3}\pi \in \mathrm{X} \tag{2}$$

where $\epsilon = \mathcal{N}\, r^3$ is the crack density parameter defined by Budianski and O'Connell (1976), $\mathcal{N}$ being the number of cracks (fractures) per unit volume. Adopting a random distribution for fractures in the medium, the Mori-Tanaka scheme provides the fallowing homogenized stiffness tensor (Maghous et al., 2014):

$$\mathbb{C}^{hom} = \lim_{\mathrm{X}\to 0}\left\{\mathbb{C}_s + \overline{\mathbb{C}_j : \left[\mathbb{I} + \mathbb{P}_G : \left(\mathbb{C}_s - \mathbb{C}_j\right)\right]^{-1}}\right\} : \left\{\mathbb{I} + \overline{\left[\mathbb{I} + \mathbb{P}_G : \left(\mathbb{C}_s - \mathbb{C}_j\right)\right]^{-1}}\right\}^{-1} \tag{3}$$

where $\mathbb{P}$ is the Hill's tensor wrote in global coordinates (see Dutra ,2012). It depends on the aspect ratio X of the oblate spheroid and its orientation $\underline{n}$. The components of the Hill tensor of an oblate spheroid can be found in Handbooks (see for instance Nemat-Nasser and Hori 1993; Mura, 1997). The symbol $\overline{\mathcal{Q}}$ denotes the integral over the spherical angular coordinates $\theta \in [0,\pi]$ and $\varphi \in [0,2\pi]$:

$$\overline{\mathcal{Q}} = \int_0^{\pi} \int_0^{2\pi} f\ \psi(\theta,\varphi)\ \mathcal{Q}(\theta,\varphi) \sin\theta\, d\theta\, d\varphi \tag{4}$$

where $\psi(\theta,\varphi)$ represents the fracture distribution function (see for instance Advani and Tucker, 1987). In the case of isotropic distribution of fractures with the same radius and aspect ratio, this function reduces to the constant value of $\psi(\theta,\varphi) = 1/4\pi$. Assuming an isotropic elasticity for the matrix material, the four-order stiffness tensor $\mathbb{C}_s$ can be described by its bulk module k_s and shear module μ_s:

$$\mathbb{C}_s = 3\,k_s\ \mathbb{J} + 2\,\mu_s\ \mathbb{K} \tag{5}$$

The fourth-order tensors $\mathbb{J}$ and $\mathbb{K}$ are defined as $\mathbb{J} = \frac{1}{3}\underline{\underline{1}} \otimes \underline{\underline{1}}$ and $\mathbb{K} = \mathbb{I} - \mathbb{J}$. Tensor $\mathbb{C}_j$ represents a four-order behavior tensor related to the crack stiffness according to:

$$\mathbb{C}_j = 3\ \mathrm{X}\ \mathrm{r}\left(k_n - \frac{4}{3}k_t\right)\mathbb{J} + 2\ \mathrm{X}\ \mathrm{r}\ k_t\ \mathbb{K} \tag{6}$$

At the macroscopic level, the effective medium is elastically isotropic. Hence,

$$\mathbb{C}^{\mathrm{hom}} = 3k_{\mathrm{hom}}\ \mathbb{J} + 2\mu_{\mathrm{hom}}\ \mathbb{K} \tag{7}$$

where k_{hom} and μ_{hom} are respectively the homogenized bulk and shear modulus. Their expressions have been derived analytically in Maghous et al. (2014) or Aguiar (2016):

$$\begin{aligned} k_{\mathrm{hom}} &= 3k_s \frac{\beta_1}{\beta_2} \\ \mu_{\mathrm{hom}} &= 45\mu_s \frac{\beta_1\beta_3}{\beta_4} \end{aligned} \tag{8}$$

β_i are coefficients that depending of matrix and fractures parameters:

$$\begin{aligned} \beta_1 &= 3\,k_s\ \pi\ \mu_s + 3\,k_s\ r\ k_n + 4\ \mu_s\ r\ k_n + \pi\ \mu_s{}^2 \\ \beta_2 &= 12\ k_s{}^2 \epsilon\ \pi + 16\ k_s\ \epsilon\ \pi\ \mu_s + 12\ r\ \mu_s\ k_n + 9\ k_s\ r\ k_n + 3\ \pi\ \mu_s{}^2 + 9\ k_s\ \pi\ \mu_s \\ \beta_3 &= 9\ k_s\ \pi\ \mu_s + 12\ k_s\ r\ k_t + 16\ \mu_s\ r\ k_t + 6\ \pi\ \mu_s{}^2 \\ \beta_4 &= \left(288\beta_1 k_s\ \mu_s \epsilon\ \pi + 384\beta_1\ \mu_s^2 \epsilon\ \pi + 48\beta_3 k_s\ \mu_s \epsilon\ \pi + 64\beta_3\ \mu_s^2 \epsilon\ \pi + 45\beta_1\beta_3\right) \end{aligned} \tag{9}$$

3 VISCOELASTIC BEHAVIOR OF FRACTURED MATERIALS

The behavior of homogenized viscoelastic materials can be derived directly from a combination of the correspondence theorem (Le et al., 2008) with the Eshelby-based elastic homogenization. The correspondence principle consists in introducing the Carson-Laplace transform in order to formulate the viscoelastic problem in terms of an equivalent elastic problem in the Laplace-domain (Bland, 1960; Salençon, 2009). The Carson-Laplace transform u^* of function u is defined by:

$$\mathrm{u}^*(p) = \int_{-\infty}^{\infty} \dot{u}(t) e^{-pt} dt \tag{10}$$

In the context of an isotropic viscoelastic-fractured material, the correspondence principle is used taking advantage of the homogenized elastic formulated in the previous section by Eq. (7) to (9) expressed in the Laplace-domain. The homogenized viscoelastic relaxation tensor is the viscous counterpart of Eq. (7):

$$\mathbb{R}^*_{hom} = \mathbb{C}^*_{hom} = 3\, k^*_{hom}\ \mathbb{J} + 2\, \mu^*_{hom}\ \mathbb{K} \tag{11}$$

where k^*_{hom} and μ^*_{hom} are respectively the homogenized bulk modulus and shear modulus Carson-Laplace transforms:

$$\begin{aligned} k^*_{hom} &= 3\, k^*_s \frac{\beta^*_1}{\beta^*_2} \\ \mu^*_{hom} &= \mu^*_s \frac{45 \beta^*_1 \beta^*_3}{\beta^*_4} \end{aligned} \tag{12}$$

It is observed that k^*_s and μ^*_s are respectively the bulk and shear moduli of matrix material in the operational space. Their values are dependent on the rheological model utilized adopted for the viscoelastic behavior of matrix material. If the Kelvin-Voigt rheological model (represented in the Fig. 3) is adopted for instance, moduli k^*_s and μ^*_s take the fallowing form:

$$\begin{aligned} k^*_s &= \frac{k^e_{m,s}\left(p\, k^v_{K,s} + k^e_{K,s}\right)}{p\, k^v_{K,s} + k^e_{K,s} + k^e_{m,s}} \\ \mu^*_s &= \frac{\mu^e_{m,s}\left(p\, \mu^v_{K,s} + \mu^e_{K,s}\right)}{p\, \mu^v_{K,s} + \mu^e_{K,s} + \mu^e_{m,s}} \end{aligned} \tag{13}$$

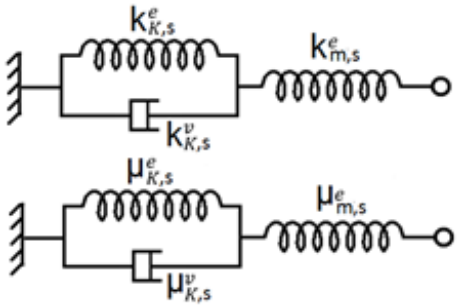

Figure 3: Kelvin-Voigt rheological model

The coefficients β_i^* are the viscous counterpart of Eq. (9):

$$\begin{aligned}
\beta_1^* &= 3\,k_s^*\,\pi\,\mu_s^* + 3\,k_s^*\,r\,k_n^* + 4\,\mu_s^*\,r\,k_n^* + \pi\,\mu_s^{*2} \\
\beta_2^* &= 12\,k_s^{*2}\epsilon\,\pi + 16\,k_s^*\,\epsilon\,\pi\,\mu_s^* + 12\,r\,\mu_s^*\,k_n^* + 9\,k_s^*\,r\,k_n^* + 3\,\pi\,\mu_s^{*2} + 9\,k_s^*\,\pi\,\mu_s^* \\
\beta_3^* &= 9\,k_s^*\,\pi\,\mu_s^* + 12\,k_s^*\,r\,k_t^* + 16\,\mu_s^*\,r\,k_t^* + 6\,\pi\,\mu_s^{*2} \\
\beta_4^* &= \left(288\beta_1^* k_s^*\,\mu_s^*\epsilon\,\pi + 384\beta_1^*\,\mu_s^{*2}\epsilon\,\pi + 48\beta_3^* k_s^*\,\mu_s^*\epsilon\,\pi + 64\beta_3^*\,\mu_s^{*2}\epsilon\,\pi + 45\beta_1^*\beta_3^*\right)
\end{aligned} \tag{14}$$

where k_n^* and k_t^* are the Carson-Laplace transforms of normal and tangential stiffness of fractures. It is observed that no restriction has been introduced regarding the rheological model of fractures, For convenience, the following notations will be introduced in the subsequent analysis:

$$\begin{aligned}
\mathrm{k}_j^* &= \mathrm{k}_n^* - \frac{4}{3}\mathrm{k}_t^* \\
\mu_j^* &= \mathrm{k}_t^*
\end{aligned} \tag{15}$$

A main issue of viscoelastic homogenization is connected with the ability to derive analytical expression for homogenized relaxation tensor from inverse Carson-Laplace transform of $\mathbb{R}_{hom}^*$. For this purpose, a specific analytical procedure is developed in the next section.

3.1 Procedure for inverse of Carson-Laplace transform

Le et al. (2008) presented a procedure to obtain the inverse Carson-Laplace transform that is valid for generalized Maxwell and generalized Kelvin rheological models. The present approach has been developed independently of the latter procedure and covers a larger number of individual rheological models adopted for matrix material and fracture material, including Spring elastic model, Maxwell model, three-element standard model, Burger model or Generalized Maxwell model. For sake of simplicity, rheological models which do not exhibit instantaneous elasticity, such as the two-element Kelvin model, shall not be considered in the present analysis.

It may be perceived from the analysis of Eq. (12) and Eq. (14) that the expressions of the bulk and shear moduli can always be written as a ratio of two polynomial functions of variable p. Referring either to k_{hom}^* or μ_{hom}^* by the generic relaxation function on R_{hom}^*, it follows that:

$$\mathrm{R}^{*}_{hom} = \frac{A(p)}{B(p)} \tag{16}$$

where polynomials $A(p)$ and $B(p)$ can be generally expressed as

$$\begin{aligned} \mathrm{A(p)} &= \sum_{k=0}^{n} a_k \, p^k \\ \mathrm{B(p)} &= \sum_{k=0}^{n} b_k \, p^k = \prod_{k=1}^{z} (p - R_k)^{g_k} \quad ; \quad b_n = 1 \end{aligned} \tag{17}$$

It is observed that for most usual rheological models, k_s^* and μ_s^* (respectively k_j^* and μ_j^*) are polynomials of same degree with respect to variable p. Thus implying that the polynomials $A(p)$ and $B(p)$have the same degree. In the above definition Eq. (17) of polynomial of $B(p)$, scalar R_k is the kth roots of $B(p)$ and g_k is the degree of the kth root, while z is the number of main poles of $B(p)$.

The first step of the inverse procedure consists in introducing the Laplace transform of R_{hom} defined as $F(p) = R^{*}_{\mathrm{hom}} / p$. This operation allows to easily splitting the relaxation function into an instantaneous part and a delayed part:

$$F(p) = \frac{a_0}{p b_0} + \frac{\dfrac{1}{b_0} \displaystyle\sum_{k=1}^{n} \left[(b_0 a_k - a_0 b_k) \, p^{k-1} \right]}{B(p)} \tag{18}$$

It is observed that $b_0 = 0$ does not correspond to any usual rheological model. Using the expression Eq. (17) of $B(p)$ into Eq. (18) yields:

$$F(p) = \frac{a_0}{p b_0} + \sum_{i=1}^{z} \sum_{k=1}^{g_i} \frac{D_{i,k}}{(p - R_i)^k} \tag{19}$$

where:

$$D_{i,k} = \frac{1}{(g_i - k)!} \frac{\partial^{(g_i - k)}}{\partial p^{(g_i - k)}} \left[\frac{C(p)}{B(p)} (p - R_i)^{g_i} \right]_{p = R_i} \tag{20}$$

and

$$C(p) = \frac{1}{b_0} \sum_{k=1}^{n} \left[(b_0 a_k - a_0 b_k) \, p^{k-1} \right] \tag{21}$$

We now proceed to the inverse of Laplace transform of $F(p)$, whose expression is given by Eq. (19). It can be readily shown that:

$$R_{hom} = \mathcal{L}^{-1}\left(F\left(p\right)\right) = \left[\frac{a_0}{b_0} + \sum_{i=1}^{z}\sum_{k=1}^{g_i}\frac{D_{i,k}}{\left(k-1\right)!}t^{k-1}e^{R_i t}\right]Y\left(t\right) \tag{22}$$

where $Y\left(t\right)$ is the Heaviside step function at origin.

Although the proposed procedure includes the situation of polynomial $B\left(p\right)$ having multiple roots, this situation does not occur for usual rheological models. It will be therefore assumed in what follows that the polynomial $B\left(p\right)$ admits only simple roots ($g_k = 1$). Eq. (22) reduces thus to:

$$R_{hom} = \left[\frac{a_0}{b_0} + \sum_{k=1}^{n} D_k e^{R_k t}\right]Y\left(t\right) \tag{23}$$

with

$$D_k = \left[\frac{C\left(p\right)}{\frac{\partial B\left(p\right)}{\partial p}}\right]_{p=R_k} = \left[\frac{C\left(p\right)\left(p-R_k\right)}{B\left(p\right)}\right]_{p=R_k} \tag{24}$$

The present reasoning has been developed for isotropic homogenized materials whose relaxation tensor $\mathbb{R}^{*}_{hom}$ can be expressed by Eq. (11). The procedure can be applied to obtain the inverse Carson-Laplace transform of the bulk and shear moduli separately.

4 EXACT HOMOGENIZED VISCOELASTIC MODEL

Before further developments, it is useful to first recall the viscoelastic generalized Maxwell model. The latter is characterized by assembling several Maxwell elements in parallel together with a spring (Fig. 4).

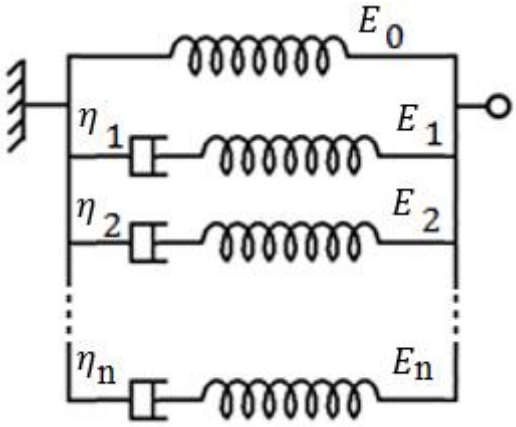

Figure 4: Generalized rheological model of Maxwell

The relaxation function R_{G-Max} associated with the generalized Maxwell model reads:

$$R_{G-Max}(t)=\left[E_0+\sum_{k=1}^{n}E_k\, e^{\left(-\frac{E_k}{\eta_k}t\right)}\right]Y(t) \tag{25}$$

which is formally identical to the homogenized relaxation of the fractured medium expressed by Eq. (23) medium, with:

$$E_0=\frac{a_0}{b_0}\quad;\quad E_k=D_k\quad;\quad -\frac{E_k}{\eta_k}=R_k\Rightarrow\eta_k=-\frac{D_k}{R_k} \tag{26}$$

This means that in the context of adopted framework, the overall viscoelastic behavior of the fractured medium can always be exactly described by an appropriate generalized Maxwell model. The homogenized isotropic behavior is characterized by:

$$\mathbb{R}_{hom}=3\,k_{hom}\;\mathbb{J}+2\,\mu_{hom}\;\mathbb{K} \tag{27}$$

where generalized Maxwell models can be associated with the bulk and the shear moduli as shown in Fig. 5.

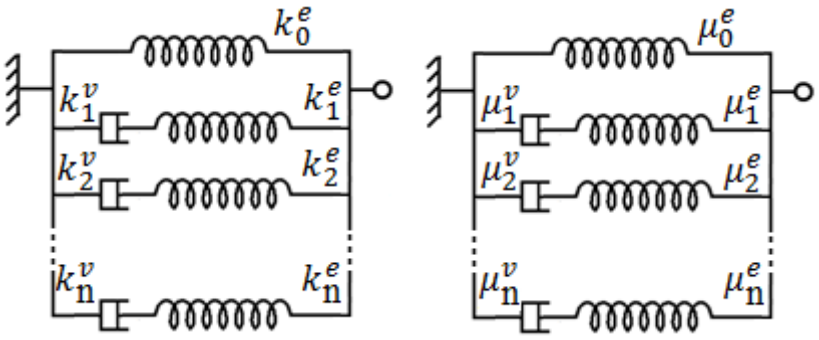

Figure 5: Generalized rheological Maxwell models for viscoelastic bulk and shear moduli.

Accordingly,

$$\begin{aligned} k_{hom}(t)&=\left[k_0^e+\sum_{k=1}^{n}k_k^e\, e^{\left(-\frac{k_k^e}{k_k^v}t\right)}\right]Y(t)\\ \mu_{hom}(t)&=\left[\mu_0^e+\sum_{k=1}^{n}\mu_k^e\, e^{\left(-\frac{\mu_k^e}{\mu_k^v}t\right)}\right]Y(t)\end{aligned} \tag{28}$$

with the following relationships:

$$\begin{aligned} k_0^e&=\frac{a_0^k}{b_0^k}\quad;\quad k_k^e=D_k^k\quad;\quad -\frac{k_k^e}{k_k^v}=R_k^k\Rightarrow k_k^v=-\frac{D_k^k}{R_k^k}\\ \mu_0^e&=\frac{a_0^\mu}{b_0^\mu}\quad;\quad \mu_k^e=D_k^\mu\quad;\quad -\frac{\mu_k^e}{\mu_k^v}=R_k^\mu\Rightarrow\mu_k^v=-\frac{D_k^\mu}{R_k^\mu}\end{aligned} \tag{29}$$

In the above expressions, superscripts k and μ are used to refer to bulk modulus and shear modulus, respectively. Parameter n in the sum operation is the number of Maxwell branches assembled in parallel with the spring. It depends on the rheological models adopted to describe the individual behaviors of matrix material and fracture material. For instance, if the Kelvin-Voigt model is used for both bulk and shear moduli of the matrix, and the fractures are assumed to behave elastically (i.e., modeled by means of springs for shear and normal behaviors), $A(p)$ and $B(p)$ are polynomials of degree four. Consequently, the value of n in Eq. (23) is equal to four, which coincides of the number of roots of polynomial $B(p)$. Consequently, the equivalent generalized Maxwell model has four branches in parallel with a spring. Changing the rheological model matrix material or fracture material will result in a different number of branches of the equivalent generalized Maxwell model.

5 SIMPLIFIED HOMOGENIZED MODEL

The whole homogenized viscoelastic behavior determined in the previous section can be described by means of Generalized Maxwell models shown in figure 4. However, it may be suitable to formulate an approximate model that would be more tractable for practical implementation in structural analyses. In the context of micromechanics approaches, Nguyen et al. (2011) developed a simplified Burger model to approximate the homogenized viscoelastic properties of a medium with cracks (i.e., discontinuities which do not able to transfer efforts). This section aims at extending the latter work to fractured viscoelastic material

Owing to isotropy at macro-scale, it is possible develop the reasoning separately for the bulk modulus and the shear modulus. For sake of simplicity, the approximate model shall be only detailed for the bulk modulus. The results regarding the shear modulus are summarized in Appendix once that the procedure to the shear module is similar. It Follows from Eq. (12) and Eq. (14) that

$$\frac{1}{k_{hom}^*} = \frac{1}{k_s^*} + \frac{4\pi\epsilon\left(3k_s^* + 4\mu_s^*\right)}{\beta_1^*} = \frac{1+\epsilon Q^*}{k_s^*} \tag{30}$$

with:

$$Q^* = \frac{4\pi\left(3k_s^* + 4\mu_s^*\right)k_s^*}{\beta_1^*} \tag{31}$$

Assuming for instance a Burger model for the behavior of the matrix material together with a Maxwell model for the fracture material, the coefficients k_s^*, μ_s^*, k_j^* and μ_j^* take the values:

$$\begin{aligned} &\frac{1}{k_s^*} = \frac{1}{k_{M,s}^{\mathrm{e}}} + \frac{1}{p\,k_{M,s}^{\mathrm{v}}} + \frac{1}{k_{K,s}^{\mathrm{e}} + p\,k_{K,s}^{\mathrm{v}}} \quad ; \quad \frac{1}{\mu_s^*} = \frac{1}{\mu_{M,s}^{\mathrm{e}}} + \frac{1}{p\,\mu_{M,s}^{\mathrm{v}}} + \frac{1}{\mu_{K,s}^{\mathrm{e}} + p\,\mu_{K,s}^{\mathrm{v}}} \\ &\frac{1}{k_j^*} = \frac{1}{k_{M,j}^{\mathrm{e}}} + \frac{1}{p\,k_{M,j}^{\mathrm{v}}} \quad ; \quad \frac{1}{\mu_j^*} = \frac{1}{\mu_{M,j}^{\mathrm{e}}} + \frac{1}{p\,\mu_{M,j}^{\mathrm{v}}} \end{aligned} \tag{32}$$

It should be kept in mind that the Carson-Laplace transform of the relaxation function K_{Bur} associated with the Burger model shown in Fig. 6 is computed as:

$$\frac{1}{k^*_{Bur}} = \frac{1}{k^{\mathrm{e}}_{M,Bur}} + \frac{1}{p\,k^{\mathrm{v}}_{M,\mathrm{Bur}}} + \frac{1}{k^{\mathrm{e}}_{K,\mathrm{Bur}} + p\,k^{\mathrm{v}}_{K,Bur}} \tag{33}$$

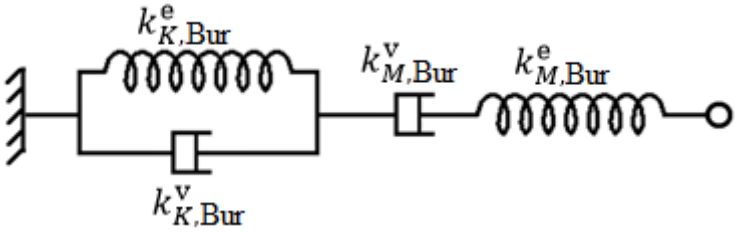

Figure 6: Burger rheological model approximating the homogenized the bulk modulus

Comparing Eq. (30) and Eq. (33) indicates that is impossible establish a direct relationship between the exact model and that associated with the Burger model. The idea to solve this problem consists in expanding in series Eq. (30) and Eq. (33) to formulate an approximation of k^*_{hom} given in Eq. (30) by the Burger model represented in Eq. (33). The approximate model is chosen such that it represents a good approximation at short $t=0$ and long $t=\infty$ times. The series expansion of Q^* at $p=0$ $(t=\infty)$ yields:

$$Q^* = Q^0_0 + Q^0_1\, p + O\left(p^2\right) \tag{34}$$

with

$$\begin{aligned}
Q^0_0 &= \frac{4\pi\, k^{\nu}_{M,s}\left(3k^{\nu}_{M,s}+4\mu^{\nu}_{M,s}\right)}{3\pi\mu^{\nu}_{M,s}\left(3k^{\nu}_{M,s}+\mu^{\nu}_{M,s}\right)+a\left(3\mu^{\nu}_{M,s}k^{\nu}_{M,j}+3k^{\nu}_{M,s}\mu^{\nu}_{M,j}+4\mu^{\nu}_{M,s}\mu^{\nu}_{M,j}\right)}\\
Q^0_1 &= \frac{4\pi\, k^{\nu}_{M,s}\left(\frac{P_1}{3}\mu^{e}_{K,s}\mu^{e}_{M,s}\mu^{e}_{M,j}\left(3k^{\nu}_{M,s}+4\mu^{\nu}_{M,s}\right)P_2+P_3\right)}{k^{e}_{M,s}k^{e}_{K,s}\mu^{e}_{M,s}\mu^{e}_{K,s}k^{e}_{M,j}\mu^{e}_{M,j}\left(P_1\right)^2}\\
P_1 &= \left(3\pi\mu^{\nu}_{M,s}\left(3k^{\nu}_{M,s}+\mu^{\nu}_{M,s}\right)+a\left(3k^{\nu}_{M,s}+4\mu^{\nu}_{M,s}\right)\left(3k^{\nu}_{M,j}+4\mu^{\nu}_{M,j}\right)\right)\\
P_2 &= \left(3k^{e}_{K,s}k^{\nu}_{M,s}k^{e}_{M,j}-3k^{e}_{K,s}k^{e}_{M,s}k^{\nu}_{M,j}+4k^{e}_{K,s}k^{e}_{M,s}\mu^{\nu}_{M,j}+3k^{e}_{K,s}k^{\nu}_{M,s}k^{e}_{M,j}\right)\\
P_3 &= -3\pi k^{e}_{K,s}k^{\nu}_{M,j}k^{e}_{M,s}\mu^{e}_{K,s}\mu^{e}_{M,j}\mu^{e}_{M,s}\mu^{\nu}_{M,s}\left(3k^{\nu}_{M,s}+4\mu^{\nu}_{M,s}\right)\left(3k^{\nu}_{M,s}+\mu^{\nu}_{M,s}\right)\\
&\quad+\frac{4}{3}ak^{e}_{K,s}k^{e}_{M,s}\mu^{e}_{K,s}{\mu^{\nu}_{M,j}}^2\mu^{e}_{M,s}\left(3k^{\nu}_{M,s}+4\mu^{\nu}_{M,s}\right)\left(3k^{e}_{M,j}+4\mu^{e}_{M,j}\right)\\
&\quad+36\pi k^{e}_{K,s}k^{e}_{M,s}{k^{\nu}_{M,s}}^2\mu^{e}_{K,s}\mu^{e}_{M,j}\mu^{\nu}_{M,j}\mu^{e}_{M,s}\mu^{\nu}_{M,s}+60\pi k^{e}_{K,s}k^{e}_{M,s}k^{\nu}_{M,s}\mu^{e}_{K,s}\mu^{e}_{M,j}\mu^{\nu}_{M,j}\mu^{e}_{M,s}{\mu^{\nu}_{M,s}}^2\\
&\quad+16\pi k^{e}_{K,s}k^{e}_{M,s}\mu^{e}_{K,s}\mu^{e}_{M,j}\mu^{\nu}_{M,j}\mu^{e}_{M,s}{\mu^{\nu}_{M,s}}^3+18\pi k^{e}_{K,s}k^{e}_{M,j}k^{e}_{M,s}\mu^{e}_{M,j}\left(\mu^{e}_{K,s}+\mu^{e}_{M,s}\right)k^{\nu}_{M,s}{\mu^{\nu}_{M,s}}^3\\
&\quad+27\pi k^{e}_{M,j}\mu^{e}_{M,j}{k^{\nu}_{M,s}}^2{\mu^{\nu}_{M,s}}^2\left(k^{e}_{K,s}k^{e}_{M,s}\mu^{e}_{K,s}+k^{e}_{K,s}k^{e}_{M,s}\mu^{e}_{M,s}+k^{e}_{K,s}\mu^{e}_{K,s}\mu^{e}_{M,s}+k^{e}_{M,s}\mu^{e}_{K,s}\mu^{e}_{M,s}\right)\\
&\quad+12\pi k^{e}_{K,s}k^{e}_{M,j}k^{e}_{M,s}\mu^{e}_{M,j}\left(\mu^{e}_{K,s}+\mu^{e}_{M,s}\right){\mu^{\nu}_{M,s}}^4
\end{aligned} \tag{35}$$

Developing Q^* at the neighbor of $p=\infty$ $(t=0)$ yields:

$$Q^* = Q_0^\infty + \frac{Q_{-1}^\infty}{p} + O\left(\frac{1}{p^2}\right) \tag{36}$$

with

$$\begin{aligned}
Q_0^\infty &= \frac{4\pi k_{M,s}^e \left(3k_{M,s}^e + 4\mu_{M,s}^e\right)}{3\pi\mu_{M,s}^e \left(3k_{M,s}^e + \mu_{M,s}^e\right) + a\left(3k_{M,s}^e k_{M,j}^e + 12\mu_{M,s}^e k_{M,j}^e + 12k_{M,s}^e \mu_{M,j}^e + 16\mu_{M,s}^e \mu_{M,j}^e\right)} \\
Q_{-1}^\infty &= \frac{4\pi k_{M,s}^e \left(\frac{1}{3}\mu_{K,s}^v \mu_{M,s}^v \mu_{M,j}^v \left(3k_{M,s}^e + 4\mu_{M,s}^e\right) S_1 S_2 + S_3\right)}{k_{M,s}^v k_{K,s}^v \mu_{M,s}^v \mu_{K,s}^v k_{M,j}^v \mu_{M,j}^v \left(S_1\right)^2} \\
S_1 &= \left(3\pi\mu_{M,s}^e \left(3k_{M,s}^e + \mu_{M,s}^e\right) + a\left(3k_{M,s}^e + 4\mu_{M,s}^e\right)\left(3k_{M,j}^e + 4\mu_{M,j}^e\right)\right) \\
S_2 &= \left(3k_{K,s}^v k_{M,s}^e k_{M,j}^v + 3k_{M,s}^v k_{M,s}^e k_{M,j}^v + 4k_{K,s}^v k_{M,s}^v \mu_{M,j}^e - 3k_{K,s}^v k_{M,s}^v k_{M,j}^e\right) \\
S_3 &= -\pi k_{K,s}^v k_{M,s}^v \mu_{K,s}^v \mu_{M,j}^v \mu_{M,s}^v \mu_{M,s}^e \left(3k_{M,s}^e + 4\mu_{M,s}^e\right)\left(3k_{M,s}^e + \mu_{M,s}^e\right)\left(3k_{M,j}^e - 4\mu_{M,j}^e\right) \\
&\quad + \frac{4}{3} a k_{K,s}^v k_{M,s}^v \mu_{K,s}^v \mu_{M,j}^{e\,2} \mu_{M,s}^v \left(3k_{M,s}^e + 4\mu_{M,s}^e\right)\left(3k_{M,j}^v + 4\mu_{M,j}^v\right) \\
&\quad - 6\pi k_{M,j}^v \mu_{M,j}^v \mu_{M,s}^{e\,2} k_{K,s}^v k_{M,s}^v \mu_{M,s}^e \left(\mu_{M,s}^v + \mu_{K,s}^v\right)\left(3k_{M,s}^e + 2\mu_{M,s}^e\right) \\
&\quad - 27\pi k_{M,j}^v \mu_{M,j}^v \mu_{M,s}^{e\,2} k_{M,s}^{e\,2} \left(\mu_{K,s}^v \mu_{M,s}^v \left(k_{K,s}^v + k_{M,s}^v\right) + k_{M,s}^v k_{K,s}^v \left(\mu_{K,s}^v + \mu_{M,s}^v\right)\right)
\end{aligned} \tag{37}$$

Expanding the equation of k_s^* on Eq. (32) leads to:

$$\begin{aligned}
p=0: &\quad \frac{1}{k_s^*} = \frac{1}{p\,k_{M,s}^v} + \left(\frac{1}{k_{M,s}^e} + \frac{1}{k_{K,s}^e}\right) + O(p) \\
p=\infty: &\quad \frac{1}{k_s^*} = \frac{1}{k_{M,s}^e} + \frac{1}{p}\left(\frac{1}{k_{M,s}^v} + \frac{1}{k_{K,s}^v}\right) + O\left(\frac{1}{p^2}\right)
\end{aligned} \tag{38}$$

Introducing the previous equations within Eq. (30), one obtains:

$$\begin{aligned}
p=0: &\quad \frac{1}{k_{hom}^*} = \frac{1+\epsilon Q_0^0}{p k_{M,s}^v} + \left(\frac{\epsilon Q_1^0}{k_{M,s}^v} + \left(1+\epsilon Q_0^0\right)\left(\frac{1}{k_{M,s}^e} + \frac{1}{k_{K,s}^e}\right)\right) + O(p) \\
p=\infty: &\quad \frac{1}{k_{hom}^*} = \frac{1+\epsilon Q_0^\infty}{k_{M,s}^e} + \frac{1}{p}\left(\left(1+\epsilon Q_0^\infty\right)\left(\frac{1}{k_{M,s}^v} + \frac{1}{k_{K,s}^v}\right) + \frac{\epsilon Q_{-1}^\infty}{k_{M,s}^e}\right) + O\left(\frac{1}{p^2}\right)
\end{aligned} \tag{39}$$

These equations must be compared with the series expansion of the Eq. (33):

$$
\begin{aligned}
&p=0: \quad \frac{1}{k_{Bur}^{*}}=\frac{1}{p\,k_{M,\mathrm{Bur}}^{v}}+\left(\frac{1}{k_{M,\mathrm{Bur}}^{e}}+\frac{1}{k_{K,\mathrm{Bur}}^{e}}\right)+O(p)\\
&p=\infty: \quad \frac{1}{k_{Bur}^{*}}=\frac{1}{k_{M,\mathrm{Bur}}^{e}}+\frac{1}{p}\left(\frac{1}{k_{M,Bur}^{v}}+\frac{1}{k_{K,Bur}^{v}}\right)+O\left(\frac{1}{p^{2}}\right)
\end{aligned}
\tag{40}
$$

The parameters defining the Burger model are thus obtained from the comparison between Eq. (39) and Eq. (40):

$$
\begin{aligned}
&\frac{1}{k_{M,Bur}^{e}}=\frac{1+\epsilon\,Q_{M}^{e}}{k_{M,s}^{e}} \quad ; \quad \frac{1}{k_{K,\mathrm{Bur}}^{e}}=\frac{1+\epsilon\,Q_{K}^{e}}{k_{K,s}^{e}}\\
&\frac{1}{k_{M,Bur}^{v}}=\frac{1+\epsilon\,Q_{M}^{v}}{k_{M,s}^{v}} \quad ; \quad \frac{1}{k_{K,Bur}^{v}}=\frac{1+\epsilon\,Q_{K}^{v}}{k_{K,s}^{v}}
\end{aligned}
\tag{41}
$$

where

$$
\begin{aligned}
&Q_{M}^{e}=Q_{0}^{\infty} \quad ; \quad Q_{K}^{e}=Q_{0}^{0}+\frac{k_{K,s}^{e}}{k_{M,s}^{v}}Q_{1}^{0}-\frac{k_{K,s}^{e}}{k_{M,s}^{e}}\left(Q_{0}^{\infty}-Q_{0}^{0}\right)\\
&Q_{M}^{v}=Q_{0}^{0} \quad ; \quad Q_{K}^{v}=Q_{0}^{\infty}+\frac{k_{K,s}^{v}}{k_{M,s}^{e}}Q_{-1}^{\infty}-\frac{k_{K,s}^{v}}{k_{M,s}^{v}}\left(Q_{0}^{0}-Q_{0}^{\infty}\right)
\end{aligned}
\tag{42}
$$

which defines entirely the bulk modulus of the Burger model approximating the homogenized material. To complete the approach, it is necessary solve the same problem regarding the approximation of homogenized shear modulus by a Burger model:

$$
\frac{1}{\mu_{Bur}^{*}}=\frac{1}{\mu_{M,Bur}^{\mathrm{e}}}+\frac{1}{p\,\mu_{M,\mathrm{Bur}}^{\mathrm{v}}}+\frac{1}{\mu_{K,Bur}^{\mathrm{e}}+p\,\mu_{K,Bur}^{\mathrm{v}}}
\tag{43}
$$

where the homogenized coefficients are provide in appendix.

We proceed now to the assessment of accuracy of the approximate Burger model through comparison with the exact homogenized relaxation bulk modulus given by Eq. (30). For illustrative purposes, the following data will be considered:

$$
\begin{aligned}
&k_{M,s}^{e}=11,4.10^{9}\,Pa \;\; ; \; k_{K,s}^{e}=9,7.10^{9}\,Pa \quad ; \; k_{M,s}^{v}=9000.10^{18}\,Pa.s \;\; ; \; k_{K,s}^{v}=95.10^{18}\,Pa.s\\
&\mu_{M,s}^{e}=8,51.10^{9}\,Pa \;\; ; \; \mu_{K,s}^{e}=7,28.10^{9}\,Pa \;\; ; \; \mu_{M,s}^{v}=6750.10^{18}\,Pa.s \;\; ; \; \mu_{K,s}^{v}=71,3.10^{18}\,Pa.s\\
&k_{M,j}^{e}=12.10^{12}\,\frac{Pa}{m} \quad ; \; k_{M,j}^{v}=120.10^{21}\,\frac{Pa}{m}.s \;\; ; \; \mu_{M,j}^{e}=10.10^{12}\,\frac{Pa}{m} \quad ; \; \mu_{M,j}^{v}=90.10^{21}\,\frac{Pa}{m}.s\\
&k_{K,j}^{e}=6.10^{12}\,\frac{Pa}{m} \;\; ; \; k_{K,j}^{v}=60.10^{21}\,\frac{Pa}{m}.s \;\; ; \; \mu_{K,j}^{e}=5.10^{12}\,\frac{Pa}{m} \;\; ; \; \mu_{K,j}^{v}=50.10^{21}\,\frac{Pa}{m}.s \;\; ; \; \epsilon=0,1
\end{aligned}
\tag{44}
$$

Figure 7 displays the variations of these moduli normalized by their initial value as a function of time. The maximum relative gap is not exceeding 11%, thus showing that the simplified model can provide an accurate approximation for all range of time.

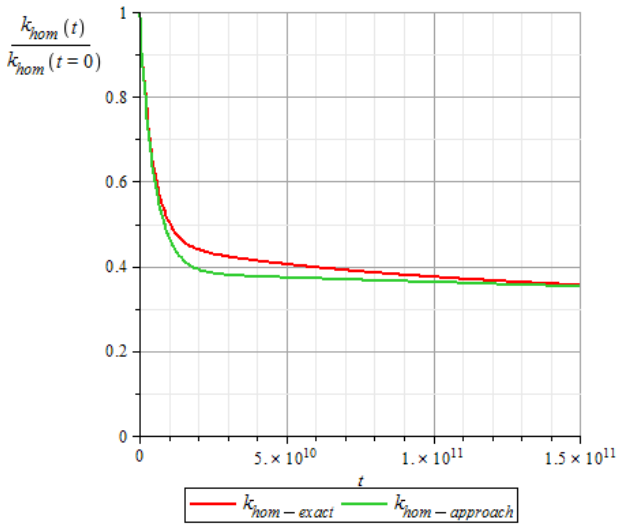

Figure 7: Homogenized bulk modulus versus time: comparison of exact and approximate Burger predictions.

Although the approach has been presented in the particular case defined by a Burger model for matrix material and a Maxell model for fracture material (Burger-Maxwell), a general procedure to formulate the approximate homogenized model has been developed for a large class of rheological models for matrix and fractures (see Table 1). However, the approximate homogenized rheological model is formulated considering it is similar to that adopted for the matrix material.

Table 1 presents the parameters required to define the individual rheological model for matrix or fractures. Subscript $\alpha = s$ refers to matrix while $\alpha = j$ refers to fractures.

Table 1: Definition of parameter used for individual models

Model	Required parameters
Crack	
Spring	$k^e_{M,\alpha}$; $\mu^e_{M,\alpha}$
Maxwell	$k^e_{M,\alpha}$; $k^v_{M,\alpha}$; $\mu^e_{M,\alpha}$; $\mu^v_{M,\alpha}$
Kelvin-Voigt	$k^e_{M,\alpha}$; $k^e_{K,\alpha}$; $k^v_{K,\alpha}$; $\mu^e_{M,\alpha}$; $\mu^e_{K,\alpha}$; $\mu^v_{K,\alpha}$
Burger	$k^e_{M,\alpha}$; $k^e_{K,\alpha}$; $k^v_{M,\alpha}$; $k^v_{K,\alpha}$; $\mu^e_{M,\alpha}$; $\mu^e_{K,\alpha}$; $\mu^v_{M,\alpha}$; $\mu^v_{K,\alpha}$

The model proposed in Nguyen et al. (2011) for a cracked medium is retrieved by considering the following parameters given in Table 2:

Table 2: Definition of parameter used to retrieve the approximate model formulated in Nguyen (2011)

Model	Used parameters
Maxwell	$k^{e}_{K,\alpha}=\infty$; $k^{v}_{K,\alpha}=\infty$; $\mu^{e}_{K,\alpha}=\infty$; $\mu^{v}_{K,\alpha}=\infty$
Kelvin-Voigt	$k^{v}_{M,\alpha}=\infty$; $\mu^{v}_{M,\alpha}=\infty$

Table 3 summarizes the different cases covered by the present modeling, as well as the maximum relative gap between the homogenized exact relaxation function and approximate equivalent model.

Table 3: Comparison of the exact and approximate homogenized bulk moduli

Matrix Model	Fracture Model	Number of Branches (Generalized Maxwell)		Equivalent approximate model	Maximum Error in approaches Model
		Bulk	Shear		
Maxwell	Crack	2	3	Maxwell	~0,00%
	Spring	3	5		~0,00%
	Maxwell	4	6		~0,00%
Kelvin-Voigt	Crack	5	6	Kelvin-Voigt	~0,00%
	Spring	5	8		0,09%
	Maxwell	7	11		11,76%
	Kelvin-Voigt	6	10		0,04%
Burger	Crack	6	8	Burger	~0,00%
	Spring	7	12		0,48%
	Maxwell	8	13		10,76%
	Kelvin-Voigt	8	14		3,12%
	Burger	10	16		9,22%

6 CONCLUSIONS

Starting from the results established in the context elastic homogenization, the effective viscoelastic properties of a fractured medium have been formulated model. The approach is based upon the combination of correspondence principle and an Eshelby-based homogenization (Mori-Tanaka) scheme. The specific inverse Carson-Laplace transform developed in this paper allows for the analytical derivation of the homogenized relaxation tensor of fractured medium. It can easily be applied for a large class of rheological models used to describe the individual viscoelastic behavior of matrix material or fracture material.

It has been shown that the overall viscoelastic behavior can always be described by an appropriate generalized Maxwell rheological model. This difference is observed in the number of branches of the model and in the value of the parameters.

Finally, an approximate model that would be more suitable for practical implementation in structural analyses has been formulated. Despite the approximate model is identified from the short and long time-term regimes, it provides accurate approximation in between these limit cases.

REFERENCES

Advani, S. G., Tucker III, C. L., 1987. The use of tensors to describe and predict fiber orientation in short fiber composites. *Journal of rheology.* vol. 31, pp. 751–784.

Aguiar, C. B., 2016. *Abordagem micromecânica da propagação de fraturas em meios elásticos e viscoelásticos*. Master's thesis, Federal University of Rio Grande do Sul/Porto Alegre.

Barton, N., Bandis, S., Bakhtar, K., 1985. Strength, deformation and conductivity coupling of rock joints. *International Journal of Rock Mechanics and Mining Sciences*, vol. 22, pp. 121–140.

Bland, D. R., 1960. *The theory of linear viscoelasticity*. Pergamon Press.

Budiansky, B., O'Connell, R. J., 1976. Elastic moduli of a cracked solid. *International Jounal of Solids Structures*, Pergamon Press, v. 12, pp. 81–97.

Dormieux, L., Kondo, D., Ulm, F. J.,2006. *Microporomechanics*. John Wiley & Sons.

Dutra, V. F. P., 2012, *Um modelo constitutivo para o concreto reforçado com fibras de aço via teoria da homogeneização*. PhD thesis, Federal Univesity of Rio Grande do Sul/Porto Alegre.

Le, Q. V., Meftah, F., He, Q. –C., Le Pape, Y., 2007. Creep and relaxation functions of a heterogeneous viscoelastic porous medium using the Mori-Tanaka homogenization scheme and a discrete microscopic retardation spectrum. *Mechanics of Time-Dependent Materials*, vol. 11, n. 3, pp. 309–331.

Maghous, S., Bernaud, D., Fréarad, J., Garnier D., 2008. Elastoplastic behavior of jointed rock masses as homogenized media and finite element analysis. *International Journal of Rock Mechanics and Mining Sciences*, vol. 45, n. 8, pp. 1273–1286.

Maghous, S., Dormieux, L., Kondo, D., Shao, J. F., 2011. Micromechanics approach to poroelastic behavior of a jointed rock. *International Journal for Numerical and Analytical Methods in Geomechanics*, vol. 37, pp. 111–129.

Maghous, S., Lorenci, G., Bittencourt E., 2014. Effective poroelastic behavior of a jointed rock. *Mechanics Research Communications*, vol. 509, pp. 54–69

Nemat-Nasser, Hori, M., 1993. *Overall properties of heterogeneous materials*. North Holland

Nguyen, S. T., 2010, *Propagation de fissures et endommagement par microfissures dans un milieu viscoélastique linéaire non vieellissant*. PhD thesis, University of Paris-Est/ Champs-sur-Marne.

Nguyen, S. T., Dormieux, L., Le Pape, Y., Sanhuja, J., 2011, A burger model for the effective behavior of a microcracked viscoelastic solid. *International Journal of Damage Mechanics*, vol. 20, n. 8, pp. 1116–1129

Nguyen, S. T., Jeannin, L., Dormieux, L L., Renard, F., 2013, Fracturing of viscoelastic geomaterials and application to sedimentary layered rocks. *Mechanics Research Communications*, vol. 49, pp. 50–56

Mura, T., 1987. *Micromechanics of defects in solids*. Kluwer Academic Publishers.

Selençon, J., 2009. Viscoélasticité pour le calcul des structures. L'École Polytechnique.

APPENDIX: COEFFICIENTS OF THE APPROACH RHEOLOGICAL MODEL OF BURGER

Expression of the relaxation function in shear associated with the approximate model is provided herein. The principle of determination is quite to that followed for the bulk relaxation modulus.

$$\begin{aligned}
&\frac{1}{\mu^e_{M,hom}} = \frac{1+\epsilon M^e_M}{\mu^e_{M,s}} \quad ; \quad \frac{1}{\mu^e_{K,hom}} = \frac{1+\epsilon M^e_K}{\mu^e_{K,s}} \\
&\frac{1}{\mu^v_{M,hom}} = \frac{1+\epsilon M^v_M}{\mu^v_{M,s}} \quad ; \quad \frac{1}{\mu^v_{K,hom}} = \frac{1+\epsilon M^v_K}{\mu^v_{K,s}}
\end{aligned} \tag{A.1}$$

with

$$\begin{aligned}
&M^e_M = M^\infty_0 \quad ; \quad M^e_K = M^0_0 + \frac{\mu^e_{K,s}}{\mu^v_{M,s}} M^0_1 - \frac{\mu^e_{K,s}}{\mu^e_{M,s}}\left(M^\infty_0 - M^0_0\right) \\
&M^v_M = M^0_0 \quad ; \quad M^v_K = M^\infty_0 + \frac{\mu^v_{K,s}}{\mu^e_{M,s}} M^\infty_{-1} - \frac{\mu^v_{K,s}}{\mu^v_{M,s}}\left(M^0_0 - M^\infty_0\right)
\end{aligned} \tag{A.2}$$

and

$$\begin{aligned}
&M^0_0 = \frac{16}{5}\frac{\pi\mu^v_{M,s}\left(3k^v_{M,s}+4\mu^v_{M,s}\right)P_3}{P_1P_2} \quad ; \quad M^0_1 = -\frac{16}{5}\frac{\pi\mu^v_{M,s}P_5}{\mu^e_{K,s}\mu^e_{M,s}k^e_{K,s}k^e_{M,s}k^e_{M,j}\mu^e_{M,j}P_4^2P_2^2} \\
&M^\infty_0 = \frac{16}{5}\frac{\pi\mu^e_{M,s}\left(3k^e_{M,s}+4\mu^e_{M,s}\right)Q_3}{Q_1Q_2} \quad ; \quad M^\infty_{-1} = \frac{16}{5}\frac{\pi\mu^e_{M,s}Q_5}{\mu^v_{K,s}\mu^v_{M,s}k^v_{K,s}k^v_{M,s}k^v_{M,j}\mu^v_{M,j}Q_4^2Q_2^2}
\end{aligned} \tag{A.3}$$

where

$$\begin{aligned}
&P_5 = U_3P_2^3 + U_2P_2^2 + U_1P_2 + U_0 \quad ; \quad Q_5 = V_3Q_2^3 + V_2Q_2^2 + V_1Q_2 + V_0 \\
&P_1 = 3\pi\mu^v_{M,s}\left(3k^v_{M,s}+\mu^v_{M,s}\right) + r\left(k^v_{M,j}k^v_{M,s} + 12k^v_{M,j}\mu^v_{M,s} + 12\mu^v_{M,s}\mu^v_{M,j} + 16\mu^v_{M,s}\mu^v_{M,j}\right) \\
&P_2 = 3\pi\mu^v_{M,s}\left(3k^v_{M,s}+2\mu^v_{M,s}\right) + 4r\mu^v_{M,j}\left(3k^v_{M,s}+4\mu^v_{M,s}\right) \\
&P_3 = \pi\mu^v_{M,s}\left(9k^v_{M,s}+4\mu^v_{M,s}\right) + 2r\left(3k^v_{M,s}+4\mu^v_{M,s}\right)\left(k^v_{M,j}+2\mu^v_{M,j}\right) \\
&P_4 = 3\pi\mu^v_{M,s}\left(3k^v_{M,s}+\mu^v_{M,s}\right) + r\left(3k^v_{M,s}+4\mu^v_{M,s}\right)\left(k^v_{M,j}+2\mu^v_{M,j}\right) \\
&Q_1 = 3\pi\mu^e_{M,s}\left(3k^e_{M,s}+\mu^e_{M,s}\right) + r\left(k^e_{M,j}k^e_{M,s} + 12k^e_{M,j}\mu^e_{M,s} + 12\mu^e_{M,s}\mu^e_{M,j} + 16\mu^e_{M,s}\mu^e_{M,j}\right) \\
&Q_2 = 3\pi\mu^e_{M,s}\left(3k^e_{M,s}+2\mu^e_{M,s}\right) + 4r\mu^e_{M,j}\left(3k^e_{M,s}+4\mu^e_{M,s}\right) \\
&Q_3 = \pi\mu^e_{M,s}\left(9k^e_{M,s}+4\mu^e_{M,s}\right) + 2r\left(3k^e_{M,s}+4\mu^e_{M,s}\right)\left(k^e_{M,j}+2\mu^e_{M,j}\right) \\
&Q_4 = 3\pi\mu^e_{M,s}\left(3k^e_{M,s}+\mu^e_{M,s}\right) + r\left(3k^e_{M,s}+4\mu^e_{M,s}\right)\left(k^e_{M,j}+2\mu^e_{M,j}\right)
\end{aligned} \tag{A.4}$$

Finally, the value of U_i and V_i are:

$$U_3 = -k^e_{K,s}k^e_{M,s}k^e_{M,\mathrm{j}}(3k^\nu_{M,s}+4\mu^\nu_{M,s})(\mu^e_{M,s}\mu^e_{K,s}(k^\nu_{M,j}+\mu^\nu_{M,\mathrm{j}})-\mu^\nu_{M,s}\mu^e_{M,\mathrm{j}}(k^e_{M,\mathrm{s}}+\mu^e_{K,\mathrm{s}}))$$

$$\begin{aligned}U_2 = {} & -\pi\mu^\nu_{M,s}(9k^\nu_{M,s}+10\mu^\nu_{M,s})U_3-\frac{1}{2}k^e_{K,s}k^\nu_{M,j}k^e_{M,s}(3k^\nu_{M,s}+4\mu^\nu_{M,s})^2.\\ & .(k^\nu_{M,j}\mu^e_{K,s}\mu^e_{M,s}(3k^e_{M,j}+2\mu^e_{M,j})-10\mu^\nu_{M,s}\mu^e_{M,j}k^e_{M,j}(\mu^e_{K,s}+\mu^e_{M,s}))\\ & +\pi k^e_{M,j}\mu^\nu_{M,s}(k^e_{K,s}k^\nu_{M,j}k^e_{M,s}\mu^e_{K,s}\mu^e_{M,s}(3k^\nu_{M,s}+4\mu^\nu_{M,s})(9k^\nu_{M,s}+5\mu^\nu_{M,s})\\ & +21k^\nu_{M,s}\mu^e_{M,j}\mu^\nu_{M,s}(k^e_{K,s}k^e_{M,s}\mu^\nu_{M,s}(\mu^e_{M,s}+\mu^e_{K,s})-k^\nu_{M,s}\mu^e_{K,s}\mu^e_{M,s}(k^e_{K,s}+k^e_{M,s})))\end{aligned}$$

$$\begin{aligned}U_1 = {} & (36\pi^2k^\nu_{M,s}(\mu^\nu_{M,s})^3+30\pi^2(\mu^\nu_{M,s})^4)U_3\\ & +6r^2k^e_{K,s}k^e_{M,j}(k^\nu_{M,j})^2k^e_{M,s}\mu^\nu_{M,s}\mu^e_{M,j}(3k^\nu_{M,s}+4\mu^\nu_{M,s})^3(\mu^e_{M,s}+\mu^e_{K,s})\\ & +9r\pi(3k^\nu_{M,s}+4\mu^\nu_{M,s})k^e_{M,j}k^\nu_{M,j}\mu^\nu_{M,s}(k^e_{K,s}k^\nu_{M,j}k^e_{M,s}\mu^e_{K,s}\mu^e_{M,s}(3k^\nu_{M,s}+4\mu^\nu_{M,s})(2\mu^\nu_{M,s}+3k^\nu_{M,s})\\ & -4\mu^e_{M,j}\mu^\nu_{M,s}((\mu^e_{M,s}+\mu^e_{K,s})(3k^e_{K,s}k^e_{M,s}k^\nu_{M,_s^2}+5k^e_{K,s}k^e_{M,s}k^\nu_{M,s}\mu^\nu_{M,s}+4k^e_{K,s}k^e_{M,s}\mu^\nu_{M,_s^2})\\ & +2(k^\nu_{M,s})^2\mu^e_{K,s}\mu^e_{M,s}(k^e_{K,s}+k^e_{M,s})))+72\pi^2(\mu^\nu_{M,s})^4(k^\nu_{M,s})^2\mu^e_{M,j}k^e_{M,j}\mu^e_{K,s}\mu^e_{M,s}(k^e_{K,s}+k^e_{M,s})\\ & -3\pi^2k^e_{K,s}k^e_{M,j}k^e_{M,s}(\mu^\nu_{M,s})^2(81k^\nu_{M,j}(k^\nu_{M,s})^3\mu^e_{K,s}\mu^e_{M,s}+234k^\nu_{M,j}(k^\nu_{M,s})^2\mu^e_{K,s}\mu^e_{M,s}\mu^\nu_{M,s}\\ & +210k^\nu_{M,j}k^\nu_{M,s}\mu^e_{K,s}\mu^e_{M,s}(\mu^\nu_{M,s})^2+56k^\nu_{M,j}\mu^e_{K,s}\mu^e_{M,s}(\mu^\nu_{M,s})^3+24k^\nu_{M,s}\mu^e_{K,s}\mu^e_{M,j}(\mu^\nu_{M,s})^3\\ & +24k^\nu_{M,s}\mu^e_{M,j}\mu^e_{M,s}(\mu^\nu_{M,s})^3)\end{aligned} \tag{A.5}$$

$$\begin{aligned}U_0 = {} & (-54\pi^3k^\nu_{M,s}(\mu^\nu_{M,s})^5-36\pi^3(\mu^\nu_{M,s})^6)U_3\\ & -18\pi r^2k^e_{M,j}(k^\nu_{M,j})^2\mu^e_{M,j}(\mu^\nu_{M,s})^2(3k^\nu_{M,s}+4\mu^\nu_{M,s})^2((\mu^e_{M,s}+\mu^e_{K,s})(9k^e_{K,s}k^e_{M,s}(k^\nu_{M,s})^2\\ & +12k^e_{K,s}k^e_{M,s}k^\nu_{M,s}\mu^\nu_{M,s}+8k^e_{K,s}k^e_{M,s}\mu^\nu_{M,_s^2})+6(k^\nu_{M,s})^2\mu^e_{K,s}\mu^e_{M,s}(k^e_{K,s}+k^e_{M,s}))\\ & -\frac{9}{2}\pi^2(3k^\nu_{M,s}+4\mu^\nu_{M,s})k^e_{M,j}k^\nu_{M,j}(\mu^\nu_{M,s})^2(3k^e_{K,s}k^\nu_{M,j}k^e_{M,s}\mu^e_{K,s}\mu^e_{M,s}(3k^\nu_{M,s}+4\mu^\nu_{M,s})(2\mu^\nu_{M,s}+3k^\nu_{M,s})^2\\ & -8(\mu^\nu_{M,s})^2\mu^e_{M,j}((\mu^e_{M,s}+\mu^e_{K,s})(9k^e_{K,s}k^e_{M,s}(k^\nu_{M,s})^2+12k^e_{K,s}k^e_{M,s}k^\nu_{M,s}\mu^\nu_{M,s}+8k^e_{K,s}k^e_{M,s}(\mu^\nu_{M,s})^2)\\ & +6(k^\nu_{M,s})^2\mu^e_{K,s}\mu^e_{M,s}(k^e_{K,s}+k^e_{M,s})))+9\pi^3k^e_{M,j}(\mu^\nu_{M,s})^4(-12(\mu^\nu_{M,s})^2\mu^e_{M,j}(k^\nu_{M,s})^2\mu^e_{K,s}\mu^e_{M,s}(k^e_{K,s}+k^e_{M,s})\\ & +k^e_{K,s}k^e_{M,s}(12k^e_{K,s}k^e_{M,s}k^\nu_{M,s}(\mu^\nu_{M,s})^3\mu^e_{M,j}(\mu^e_{M,s}+\mu^e_{K,s})\\ & +k^e_{K,s}k^\nu_{M,j}k^e_{M,s}\mu^e_{K,s}\mu^e_{M,s}(2\mu^\nu_{M,s}+3k^\nu_{M,s})(3k^\nu_{M,s}+4\mu^\nu_{M,s})(4\mu^\nu_{M,s}+9k^\nu_{M,s})))\end{aligned}$$

$$V_3 = k^v_{K,s}k^v_{M,j}k^v_{M,s}(3k^e_{M,s}+4\mu^e_{M,s})(\mu^v_{K,s}\mu^v_{M,s}(k^e_{M,j}+\mu^e_{M,j})-\mu^e_{M,s}\mu^v_{M,j}(\mu^v_{K,s}+\mu^v_{M,s}))$$

$$\begin{aligned}V_2 = \frac{1}{2}rk^v_{K,s}k^e_{M,j}k^v_{M,s}(3k^e_{M,s}+4\mu^e_{M,s})^2(&k^e_{M,j}\mu^v_{K,s}\mu^v_{M,s}(2\mu^v_{M,j}+3k^v_{M,j})\\&-10k^v_{M,j}\mu^e_{M,s}\mu^v_{M,j}(\mu^v_{K,s}+\mu^v_{M,s}))\\&-\pi k^v_{M,j}\mu^e_{M,s}(k^v_{K,s}(3k^e_{M,s}+4\mu^e_{M,s})k^v_{M,s}\mu^v_{K,s}\mu^v_{M,s}(18k^e_{M,j}k^e_{M,s}+15k^e_{M,j}\mu^e_{M,s}\\&+9k^e_{M,s}\mu^e_{M,j}+10\mu^e_{M,j}\mu^e_{M,s})-\mu^e_{M,s}\mu^v_{M,j}((\mu^v_{K,s}+\mu^v_{M,s})(27k^v_{K,s}(k^e_{M,s})^2k^v_{M,s}\\&+45k^v_{K,s}k^e_{M,s}k^v_{M,s}\mu^e_{M,s}+40k^v_{K,s}k^v_{M,s}(\mu^e_{M,s})^2)+21(k^e_{M,s})^2\mu^v_{K,s}\mu^v_{M,s}(k^v_{K,s}+k^v_{M,s})))\end{aligned}$$

$$\begin{aligned}V_1 = &-6r^2(k^e_{M,j})^2k^v_{M,j}k^v_{K,s}k^v_{M,s}\mu^e_{M,s}\mu^v_{M,j}(3k^e_{M,s}+4\mu^e_{M,s})^3(\mu^v_{K,s}+\mu^v_{M,s})\\&-9r\pi(3k^e_{M,s}+4\mu^e_{M,s})k^e_{M,j}k^v_{M,j}\mu^e_{M,s}(k^v_{K,s}k^e_{M,j}k^v_{M,s}\mu^v_{K,s}\mu^v_{M,s}(3k^e_{M,s}+4\mu^e_{M,s})(2\mu^e_{M,s}+3k^e_{M,s})\\&-4\mu^e_{M,s}\mu^v_{M,j}((\mu^v_{K,s}+\mu^v_{M,s})(3k^v_{K,s}(k^e_{M,s})^2k^v_{M,s}+5k^v_{K,s}k^e_{M,s}k^v_{M,s}\mu^e_{M,s}+4k^v_{K,s}k^v_{M,s}(\mu^e_{M,s})^2)\\&+2(k^e_{M,s})^2\mu^v_{K,s}\mu^v_{M,s}(k^v_{K,s}+k^v_{M,s})))\\&+3\pi^2k^v_{M,j}(\mu^e_{M,s})^2(k^v_{K,s}(3k^e_{M,s}+4\mu^e_{M,s})k^v_{M,s}\mu^v_{K,s}\mu^v_{M,s}(27k^e_{M,j}(k^e_{M,s})^2+54k^e_{M,j}k^e_{M,s}\mu^e_{M,s}\\&+24k^e_{M,j}(\mu^e_{M,s})^2+12k^e_{M,s}\mu^e_{M,j}\mu^e_{M,s}+10\mu^e_{M,j}(\mu^e_{M,s})^2)\\&-2(\mu^e_{M,s})^2\mu^v_{M,j}((\mu^v_{K,s}+\mu^v_{M,s})(18k^v_{K,s}(k^e_{M,s})^2k^v_{M,s}+27k^v_{K,s}k^e_{M,s}k^v_{M,s}\mu^e_{M,s}\\&+20k^v_{K,s}k^v_{M,s}(\mu^e_{M,s})^2)+12(k^e_{M,s})^2\mu^v_{K,s}\mu^v_{M,s}(k^v_{K,s}+k^v_{M,s})))\end{aligned} \tag{A.6}$$

$$\begin{aligned}V_0 = &18r^2pk^e_{M,_s^2,j}k^v_{M,j}\mu^v_{M,j}\mu^e_{M,_s^2}(3k^e_{M,s}+4\mu^e_{M,s})^2((\mu^v_{K,s}+\mu^v_{M,s})(9k^v_{K,s}k^e_{M,_s^2}k^v_{M,s}+12k^v_{K,s}k^e_{M,s}k^v_{M,s}\mu^e_{M,s}\\&+8k^v_{K,s}k^v_{M,s}\mu^e_{M,_s^2})+6k^e_{M,_s^2}\mu^v_{K,s}\mu^v_{M,s}(k^v_{K,s}+k^v_{M,s}))\\&+(9/2)p^2(3k^e_{M,s}+4\mu^e_{M,s})k^e_{M,j}k^v_{M,j}\mu^e_{M,_s^2}(3k^v_{K,s}k^e_{M,j}k^v_{M,s}\mu^v_{K,s}\mu^v_{M,s}(3k^e_{M,s}+4\mu^e_{M,s})(2\mu^e_{M,s}+3k^e_{M,s})^2\\&-8\mu^e_{M,_s^2}\mu^v_{M,j}((\mu^v_{K,s}+\mu^v_{M,s})(9k^v_{K,s}k^e_{M,_s^2}k^v_{M,s}+12k^v_{K,s}k^e_{M,s}k^v_{M,s}\mu^e_{M,s}+8k^v_{K,s}k^v_{M,s}\mu^e_{M,_s^2})\\&+6k^e_{M,_s^2}\mu^v_{K,s}\mu^v_{M,s}(k^v_{K,s}+k^v_{M,s})))\\&-9p^3k^v_{M,j}\mu^e_{M,_s^4}(k^v_{K,s}\mu^v_{K,s}\mu^v_{M,s}k^v_{M,s}(3k^e_{M,s}+4\mu^e_{M,s})(2\mu^e_{M,s}+3k^e_{M,s})(9k^e_{M,j}k^e_{M,s}+6k^e_{M,j}\mu^e_{M,s}+2\mu^e_{M,j}\mu^e_{M,s})\\&-2\mu^e_{M,_s^2}\mu^v_{M,j}((\mu^v_{K,s}+\mu^v_{M,s})(9k^v_{K,s}k^e_{M,_s^2}k^v_{M,s}+12k^v_{K,s}k^e_{M,s}k^v_{M,s}\mu^e_{M,s}+8k^v_{K,s}k^v_{M,s}\mu^e_{M,_s^2})\\&+6k^e_{M,_s^2}\mu^v_{K,s}\mu^v_{M,s}(k^v_{K,s}+k^v_{M,s})))\end{aligned}$$